Aalborg Universitet

Fast Array diagnosis for Subarray Structured 5G Base Station Antennas

Mengting Li, Fengchun Zhang, Zhengpeng Wang and Wei Fan

Abstract—Antenna array composed of subarrays is a widely-used array structure in the fifth generation (5G) base stations (BSs), which can offer both high gain beam and beam-steering capability. Generally, subarray-structured BS antennas consist of a number of subarrays, each composed of a few antenna elements, making the array diagnosis a pronounced and challenging problem. A fast diagnosis method, which can be conducted in the near-field of the BS array is presented for BS array of subarrays (AoSAs) in this letter. The objective is to detect antenna failures, which can be caused by the disconnection at either the feed of subarray or the feed of antenna element in the subarray, based on complex array signals recorded by only a few probes with a short measurement distance. The diagnosis is achieved by a novel two-stage measurement procedure based on solving linear equations. Finally, an array composed of 4 subarrays with 24 antenna elements in total was used to validate the effectiveness and robustness of the proposed method in a practical setup.

Index Terms—array diagnosis, array of subarrays (AoSAs), antenna measurement, BS antennas.

Fig. 1. The diagram of the structure of AoSA with wide (with switch-off) and narrow-beam mode (with switch-on).

I. Introduction

THE rectangular antenna array composed of a number of subarrays is a prevalent array structure employed in the fifth generation (5G) base stations (BSs) [1]–[3]. The planar BS array consists of several subarrays, each of which composed of a few antenna elements, as illustrated in Fig. 1. Given a fixed number of antenna elements in a planar array, partitioning these antennas into several subarrays can reduce the total number of required RF chains and thereby mitigate the high power consumption and integration complexity of the antennas and RF circuity. Combined with beam-forming technique, an array of subarrays (AoSAs) can provide both high gain beams and beam-steering capability. The beam-steering capability is achieved by individually controlling the amplitude and phase excitation of the subarrays. This is done by applying two dedicated radio chains per subarray (one per polarization) to enable the control. The number of elements in one subarray is typically selected as a balance between coverage and array half-power beam-width (HPBW). [4]. Typically, 5G base station antennas have up to 8 subarrays in horizontal direction yet limited in vertical direction with no more than 8 antenna elements in one subarray [5]. In this way, the direction and other radiation characteristics, e.g., beam scanning range, sidelobe level, grating lobe level etc, are managed. Moreover, to meet the requirement of various user
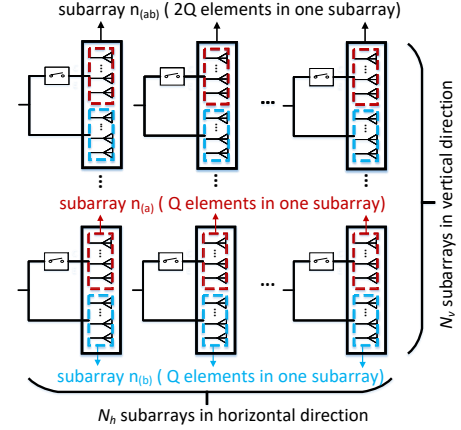
Mengting Li, Fengchun Zhang, and Wei Fan are with the Antenna Propagation and Millimeter-wave Systems (APMS) section, Aalborg University, Denmark. Zhengpeng Wang is with Electronics and Information Engineering, Beihang University, Beijing 100191, China.

Corresponding author: Wei Fan (Email: wfa@es.aau.dk).

equipment (UE) distribution scenarios (e.g. dense urban high-rise or rural scenarios) with the cost consideration, subarrays with different beam-width in the vertical direction might be integrated in one AoSAs. One practical BS array structure combining wide and narrow-beam modes in vertical direction is illustrated in Fig. 1. The narrow-beam mode, i.e. all the antenna elements in one subarray are excited (switch-on), will be implemented in low rise urban or rural areas whereas wide-beam mode, i.e. half elements in one subarray (switch-off) are excited, can be used for high rise urban area [4].

Despite the benefits provided by the AoSA, the diagnosis of these arrays can be a challenging task due to the large array size and limited tolerance in measurement time for manufactures. The data acquisition is preferred to be conducted in the near-field of the array since the far-field condition [6] of large scale arrays is difficult to fulfill in practical testing environments. Many array diagnosis methods have been proposed in the literature. Backward transformation method (BTM) [7] is a well-known diagnosis method based on the field transformation algorithms. However, large number of near-field samples, which need to fulfil the Nyquist sampling criteria, are required to obtain sufficient resolution of the reconstructed aperture field, resulting in extremely long measurement time for large scale arrays. Genetic algorithm has been implemented in [8], [9] to achieve array diagnosis based on detecting the variation of array factor using the far-field measurement data. Compressed sensing technique based methods for large scale arrays with a small number of near-field measurement samples were presented in [10]–[12], where the knowledge of a "faulty-free" array, i.e. array
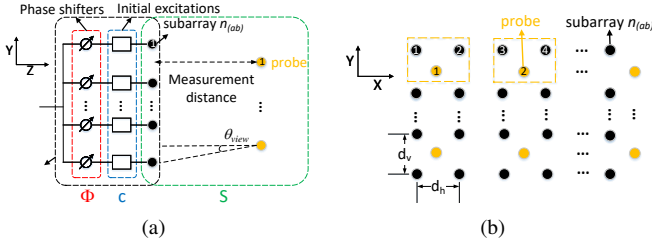
Fig. 2. (a) A schematic of the diagnosis system. (b) The layout of the AUT and probes.

without failure elements is required. The array diagnosis can also be achieved by retrieving the excitation of each antenna element. In [13], [14], the excitation of each element is retrieved by solving linear equations based on the complex array signals recorded by a single probe. However, it can only be effective for arrays composed of small size subarrays since the testing sensitivity becomes unacceptable when the number of elements within the subarray exceeds three, as discussed in Section II-B. Our proposed method can further improve the testing accuracy and sensitivity compared with the method in [13] by applying multiple probes placed in the near-field of antenna under test (AUT) and two-stage process, respectively. The proposed method does not require dedicate measurement conditions, pre-knowledge of the AUT nor large number of field samples. It is accurate, fast and effective for arrays composed of large size subarrays, making it promising for 5G BS antenna diagnosis.

In this letter, the array diagnosis for AoSAs is achieved by a novel two-stage diagnosis process based on solving linear equations. The working principle of the proposed method is firstly explained and analyzed theoretically in Section II. Then, a measurement campaign was designed and conducted to validate the effectiveness of the proposed method. Finally, the conclusion is drawn in Section IV.

II. THEORY

A. Signal model

The AUT is an AoSAs composed of $N = N_v \times N_h$ subarrays (named as subarray $n_{(ab)}$, $n \in [1, N]$), each of which contains $2Q$ antenna elements (marked as solid black rectangles in Fig. 1). Each subarray $n_{(ab)}$ can be divided into two smaller subarrays, i.e., subarray $n_{(a)}$ and subarray $n_{(b)}$, both including Q elements. All the elements are excited (switch-on) for narrow beam mode whereas only half elements, i.e., elements in the dashed blue squares, are excited (switch-off) for wide beam mode as shown in Fig. 1. Fig. 2 (a) and (b) show the schematic of the diagnosis system, and the layout of the AUT and the multi-probe, respectively. Assume that all the antenna elements in the AoSAs have the same radiation pattern. One external phase shifter is required for each subarray $n_{(ab)}$ to tune the phase into $0°$ or $180°$. Note that the external phase shifters are only used for diagnosis purpose. The signal model of the AoSA diagnosis system can be written as

$$\mathbf{\Phi} \cdot \mathbf{X} = \mathbf{Y}, \tag{1}$$

$$\mathbf{\Phi} = \begin{bmatrix} e^{j\phi_{1,1_{(\alpha)}}} & \cdots & e^{j\phi_{1,N_{(\alpha)}}} \\ \vdots & \ddots & \vdots \\ e^{j\phi_{M,1_{(\alpha)}}} & \cdots & e^{j\phi_{M,N_{(\alpha)}}} \end{bmatrix}, \tag{2}$$

$$\mathbf{X} = \begin{bmatrix} c_{1_{(\alpha)}} S_{1_{(\alpha)},1} & \cdots & c_{1_{(\alpha)}} S_{1_{(\alpha)},L} \\ \vdots & \ddots & \vdots \\ c_{N_{(\alpha)}} S_{N_{(\alpha)},1} & \cdots & c_{N_{(\alpha)}} S_{N_{(\alpha)},L} \end{bmatrix}, \tag{3}$$

$$\mathbf{Y} = \begin{bmatrix} y_{1,1_{(\alpha)}} & \cdots & y_{1,L_{(\alpha)}} \\ \vdots & \ddots & \vdots \\ y_{M,1_{(\alpha)}} & \cdots & y_{M,L_{(\alpha)}} \end{bmatrix}, \tag{4}$$

where N is the total number of subarrays, M is the number of measurements at each probe and L is the number of probes. $\mathbf{\Phi} = \{e^{j\phi_{m,n_{(\alpha)}}}\}$ is the designed phase shift setting matrix with $\phi_{m,n_{(\alpha)}}$ denoting the assigned phase shift value of the subarray $n_{(\alpha)}$ for the m-th measurement ($n \in [1, N]$, $m \in [1, M]$, $\alpha \in \{ab, b\}$). Note that subarray $n_{(ab)}$ and $n_{(b)}$ indicate the subarray operated in narrow and wide-beam mode, respectively. $\mathbf{X} = \{x_{n_{(\alpha)},l}\} = \{c_{n_{(\alpha)}} S_{n_{(\alpha)},l}\}$ with $c_{n_{(\alpha)}}$ and $S_{n_{(\alpha)},l}$ denoting the initial excitation of the subarray $n_{(\alpha)}$, and transmission coefficient between the subarray and the l-th probe antenna, respectively. $\mathbf{Y} = \{y_{m,l_{(\alpha)}}\}$ represents the complex array signals with $y_{m,l_{(\alpha)}}$ denoting the complex array signal when the array composed of subarray $n_{(\alpha)}$ is excited, measured by the l-th probe antenna of the m-th measurement.

B. Problem statement

As mentioned before, [13] proposed an effective method to obtain the relative excitation of each antenna element, which requires the phase tuning of individual antenna elements. One probe is placed in the far-field of the array to receive the complex array signals in this method. With the restriction of the present array structure shown in Fig. 1 and the near-field measurement condition, only the $x_{n_{(ab)},l} = c_{n_{(ab)}} S_{n_{(ab)},l}$ can be directly obtained by solving (1). The relative amplitude of excitation between subarray $i_{(ab)}$ and subarray $j_{(ab)}$ is $c_{i_{(ab)}}/c_{j_{(ab)}}$ ($i, j \in [1, N]$). The reliable estimation of relative excitation of subarrays can be obtained when the difference between $S_{i_{(ab)},u}$ and $S_{j_{(ab)},v}$ ($u, v \in [1, L]$) is small as (6) shows:

$$\frac{c_{i_{(ab)}}}{c_{j_{(ab)}}} = \frac{c_{i_{(ab)}} S_{i_{(ab)},u}}{c_{j_{(ab)}} S_{j_{(ab)},v}} \cdot \frac{S_{j_{(ab)},v}}{S_{i_{(ab)},u}} \approx \frac{x_{i_{(ab)},u}}{x_{j_{(ab)},v}} \tag{5}$$

Then, the diagnosis results can be achieved by comparing the estimated excitation power between subarray with failure elements and normal subarrays. However, with one probe antenna placed in the near-field and boresight of the AUT, the signals seen by the elements on the edge might be significantly attenuated since the θ_{view} (i.e., angle between the boresight direction of the probe and the direction of the subarray from the probe side) of center subarrays is much smaller than the that of edge subarrays. Such inhomogeneities among edge elements and center elements will introduce errors for the diagnosis. Moreover, even if the differences between $S_{i_{(ab)},1}$ and $S_{j_{(ab)},1}$ can be ignored, the testing sensitivity of

the system is constrained. For instance, the power difference between the subarray with one failure element and the normal subarray will only be 1.6 dB when $2Q = 6$, which makes the detection extremely difficult in a practical setup due to the unavoidable noise effect. Therefore, a more practical and effective diagnosis method for AoSAs is desired.

C. Proposed algorithm

To solve the above-discussed problems, a novel two-stage diagnosis process using multi-probes in the near-field of the array is proposed. The relative excitation power of each subarray $n_{(a)}$ and subarray $n_{(b)}$ will be obtained by performing a two-stage measurement, i.e., conducting all the measurements firstly in the wide beam working mode and then in the narrow beam working mode. The estimated relative excitation power for each subarray $n_{(a)}$ and subarray $n_{(b)}$ will finally be calculated by solving linear equations. For each measurement, a specific phase shift setting is assigned to different subarrays according to matrix $\mathbf{\Phi}$, and the complex array signal received by each probe will be recorded by VNA, i.e., $\mathbf{Y}$ matrix in the signal model. The above operation will be repeated for different phase shift settings.

The number of the required probes is $L = \lceil N_v/2 \rceil \times \lceil N_h/2 \rceil$ and their location is deliberately selected as depicted in Fig. 2 (b). Note that other layout of the multi-probe configurations can also be used as long as the transmission coefficients between different subarrays and their nearest probe are similar. In principle, the multiple probes could be placed at just the far-field of the subarray (i.e., subarray $n_{(a)}$ or subarray $n_{(b)}$). However, it is necessary to reduce the subarray gain differences in the direction of the nearest probe when the radiation pattern of the antenna element is not identical due to the mutual coupling effects. Therefore, the view angle θ_{view}, as shown in Fig. 2 (a), is better to be smaller than the half power beam width (HPBW) of the probe and AUT elements to minimize the diagnosis errors since the distortion of the radiation pattern is negligible within the range of HPBW. The detailed diagnosis process is explained as follows:

Stage I: We aim to obtain the relative amplitude of estimated excitation of subarray $n_{(b)}$, $n \in [1, N]$. Let AUT work in the wide-beam mode, i.e., only subarray $n_{(b)}$ is excited. The $x_{n_{(b)},l}$ of subarray $n_{(b)}$ can be obtained by solving linear equation shown in (1). The phase shift setting matrix $\mathbf{\Phi}$ can be selected as a Hadamard matrix or generated by three basic matrices with small condition number [13]. For simplicity, assume that we have $N = N_v \times N_h = 1 \times 4$ subarrays with $2Q = 6$ (i.e. each subarray $n_{(ab)}$ contains 6 antenna elements). $\mathbf{\Phi}$ based on Hadamard matrix can be written as

$$\mathbf{\Phi} = \begin{bmatrix} 1 & 1 & 1 & 1 \\ 1 & -1 & 1 & -1 \\ 1 & 1 & -1 & -1 \\ 1 & -1 & -1 & 1 \end{bmatrix}, \quad (6)$$

where "1" and "-1" represent $0°$ and $180°$ phase shift, respectively. Then, the $x_{n_{(b)},l}$ can be solved using (1). When the radiation pattern of the probe and subarray $n_{(b)}$ are both symmetrical in horizontal and vertical planes, we have $|S_{1_{(b)},1}| = |S_{2_{(b)},1}| = |S_{3_{(b)},2}| = |S_{4_{(b)},2}|$, as marked in the

yellow dashed square in Fig. 2 (b). The relative amplitude of excitation of subarray $n_{(b)}$ can be expressed as $|c_{1_{(b)}}| : |c_{2_{(b)}}| : |c_{3_{(b)}}| : |c_{4_{(b)}}| = |x_{1_{(b)},1}| : |x_{2_{(b)},1}| : |x_{3_{(b)},2}| : |x_{4_{(b)},2}|$. Although symmetrical radiation patterns are assumed for ease of formula derivation, the proposed method is not sensitive to pattern discrepancies since we do not require precise estimation of the relative excitation power for diagnosis purpose.

Stage II: We aim to obtain the relative amplitude of estimated excitation of subarray $n_{(a)}$, $n \in [1, N]$. Since subarray $n_{(a)}$ cannot work independently, its relative amplitude of estimated excitation of subarrays cannot be directly obtained. The basic idea is to make use of complex array signals captured by the probes when the AUT works in narrow beam mode. Let the AUT work in the narrow-beam mode. Apply the same phase shift setting matrix $\mathbf{\Phi}$ and conduct the measurements. The complex array signals $y_{m,l_{(ab)}}$ of subarray $n_{(ab)}$ are also measured by the previous two probes. Then, the complex array signals $y_{m,l_{(a)}}$ when each subarray $n_{(a)}$ is excited can be obtained by

$$y_{m,l_{(a)}} = y_{m,l_{(ab)}} - y_{m,l_{(b)}}. \quad (7)$$

The $x_{n_{(a)},l}$ and the relative amplitude of estimated excitation of each subarray $n_{(a)}$ can be obtained using the similar method in Stage I. To assist the detection, a parameter, which represents the difference of the excitation power between subarrays (i.e. subarray $n_{(a)}$ and $n_{(b)}$) with and without failure elements is defined as

$$D = -20\log_{10}\frac{Q-i}{Q}, \quad (8)$$

where i is the number of failure elements in one subarray. D can be used as a reference to determine how many failure elements are in the subarray. As the i increases, the value of D will become larger and the failure will be easier to be detected. When the size of subarray increases, the value of D decreases and the testing sensitivity reduces. However, the number of the elements in a subarray is smaller than 8 for common 5G BS antennas and the proposed method can provide acceptable testing sensitivity for these AosAs. Since we can only obtain the relative excitation power of each subarray, it is not possible to directly know the detailed location of the failure elements. However, the specific locations can be further obtained by using conventional "face-to-face" near-field scanner, i.e., comparing the received signal power using a near-field probe placed close to different elements of the identified faulty subarray.

III. MEASUREMENT VALIDATION

A. Measurement System

A measurement campaign was conducted in a typical indoor scenario to verify the proposed diagnosis method. The photo of the measurement setup is shown in Fig. 3. The required devices include the following:

1) A vector network analyzer (VNA);
2) 4 digital phase shifters with phase adjustment range of $360°$ and phase adjustment resolution of $1°$;
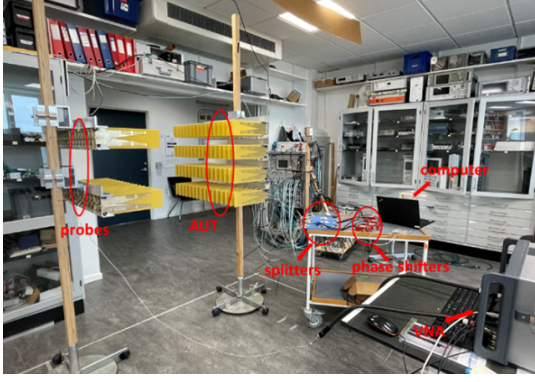3) Some horn antennas of Vivaldi type;
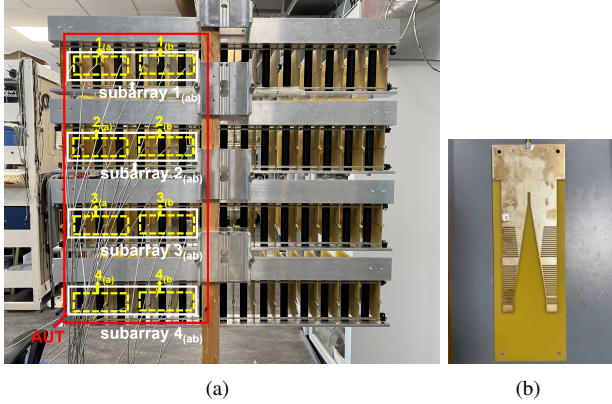4) 5 power splitters;

Fig. 3. The photo of the measurement setup.

Fig. 4. The photos of (a) AUT used in the measurement system, and (b) horn antenna of Vivaldi type.

5) A laptop which controls the phase shifters and communicates with VNA to save the recorded data.

The AUT in the real measurement contains 4 subarrays. Each subarray $n_{(ab)}$ includes 6 elements, which are selected from one row of the antenna as detailed in the Fig. 4 (a). Subarray $n_{(ab)}$ can be divided into two smaller subarrays with equal number of elements, i.e., subarray $n_{(a)}$ and subarray $n_{(b)}$. One probe is placed towards the center of subarray $1_{(ab)}$ and subarray $2_{(ab)}$ and the other probe is placed towards the center of subarray $3_{(ab)}$ and subarray $4_{(ab)}$. The working frequency band of the antenna element (shown in Fig 4 (b)) is from 2.5 GHz to 4 GHz with 9 dBi gain and 50° HPBW at 3 GHz. The element spacing within subarray $n_{(ab)}$ is 50 mm whereas the spacing between different subarrays is 150 mm. The dimensions of the whole array are 550 mm × 250 mm × 30 mm. The complex array signals received by each probe were recorded on VNA at 3 GHz. The amplitude uncertainty introduced by the digital phase shifter, power splitters and connecting cables is within ±0.8 dB. Note that the noise effects are typically not an issue in real antenna measurements since the measurement is conducted in good signaling condition with the use of VNA and small measurement distance.

B. Measurement Results

For simplicity, only two typical failure cases have been considered in the measurements, i.e. case I: one subarray
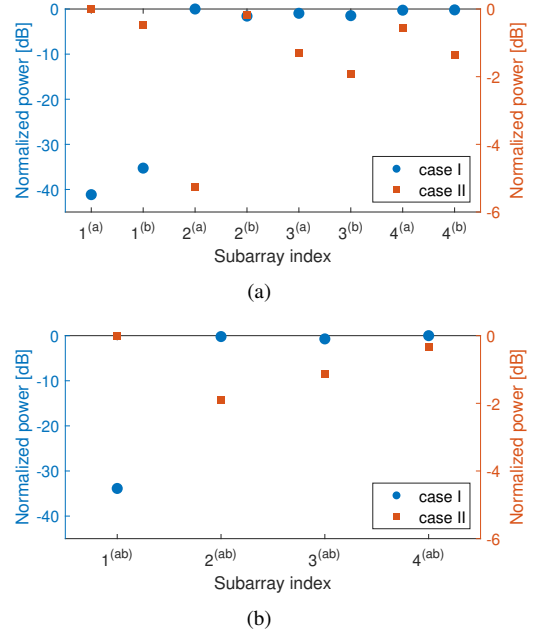

Fig. 5. The diagnosis results of the (a) proposed and (b) reference methods.

failure and case II: one antenna element failure. The failures were implemented by disconnecting the feed at the subarray $n_{(ab)}$ side or the antenna element side. Typically, we choose subarray $1_{(ab)}$ as the failure array for case I and one element failure in subarray $2_{(a)}$ for case II. The diagnosis results achieved by the proposed method is compared to that with the reference method proposed in [13], as illustrated in Fig. 5. Note that the same two probes are used in these two methods yet the proposed method can obtain the normalized excitation power of all suabrray $n_{(a)}$ and $n_{(b)}$ whereas the reference method can only get the estimation results of suabrray $n_{(ab)}$. Both the proposed method and the reference method can successfully detect the subarray failure since the normalized excitation power of the associated subarrays are all below -30 dB indicating no excitation signals. For one antenna element failure case, the proposed method can still detect the failure since the difference between the normal subarrays and subarray $2_{(a)}$ is around 3-5 dB. However, the difference between the normal subarrays and subarray $2_{(ab)}$ using the reference method is around 0.7-1.9 dB which is difficult to be detected. A more reliable array diagnosis for AoSAs can be achieved with the proposed method.

IV. CONCLUSION

In this letter, a fast array diagnosis method is proposed for AoSAs operating in both wide and narrow-beam modes. Sparse probes are placed in the near-field of the array to receive the complex array signals with designed phase shift settings. Compared to the state-of-the-art methods, this diagnosis method is reliable and efficient without requiring lots of near-field samples distributing across the whole array aperture. Measurement results show that the failure elements can be successfully detected, which validates the effectiveness of the proposed method.

REFERENCES

[1] Y. Aslan, J. Puskely, A. Roederer, and A. Yarovoy, "Active multiport sub-arrays for 5g communications," in *2019 IEEE-APS Topical Conference on Antennas and Propagation in Wireless Communications (APWC)*. IEEE, 2019, pp. 298–303.

[2] H. Chu and Y.-X. Guo, "A filtering dual-polarized antenna subarray targeting for base stations in millimeter-wave 5g wireless communications," *IEEE Transactions on Components, Packaging and Manufacturing Technology*, vol. 7, no. 6, pp. 964–973, 2017.

[3] P. von Butovitsch, D. Astely, C. Friberg, A. Furuskär, B. Göransson, B. Hogan, J. Karlsson, and E. Larsson, "Advanced antenna systems for 5g networks," *Ericsson White Paper*, 2018.

[4] W. Roh, J.-Y. Seol, J. Park, B. Lee, J. Lee, Y. Kim, J. Cho, K. Cheun, and F. Aryanfar, "Millimeter-wave beamforming as an enabling technology for 5g cellular communications: Theoretical feasibility and prototype results," *IEEE communications magazine*, vol. 52, no. 2, pp. 106–113, 2014.

[5] M. N. Hamdy, "Beamformers explained," *Commscope White Paper*, 2020.

[6] C. A. Balanis, *Antenna theory: analysis and design*. John wiley & sons, 2015.

[7] J. Lee, E. M. Ferren, D. P. Woollen, and K. M. Lee, "Near-field probe used as a diagnostic tool to locate defective elements in an array antenna," *IEEE Transactions on Antennas and Propagation*, vol. 36, no. 6, pp. 884–889, 1988.

[8] O. Bucci, A. Capozzoli, and G. D'elia, "Diagnosis of array faults from far-field amplitude-only data," *IEEE Transactions on Antennas and Propagation*, vol. 48, no. 5, pp. 647–652, 2000.

[9] J. A. Rodriguez-Gonzalez, F. Ares-Pena, M. Fernandez-Delgado, R. Iglesias, and S. Barro, "Rapid method for finding faulty elements in antenna arrays using far field pattern samples," *IEEE Transactions on Antennas and Propagation*, vol. 57, no. 6, pp. 1679–1683, 2009.

[10] M. D. Migliore, "A compressed sensing approach for array diagnosis from a small set of near-field measurements," *IEEE Transactions on Antennas and Propagation*, vol. 59, no. 6, pp. 2127–2133, 2011.

[11] B. Fuchs, L. Le Coq, and M. D. Migliore, "Fast antenna array diagnosis from a small number of far-field measurements," *IEEE Transactions on Antennas and Propagation*, vol. 64, no. 6, pp. 2227–2235, 2016.

[12] C. Xiong, G. Xiao, Y. Hou, and M. Hameed, "A compressed sensing-based element failure diagnosis method for phased array antenna during beam steering," *IEEE Antennas and Wireless Propagation Letters*, vol. 18, no. 9, pp. 1756–1760, 2019.

[13] R. Long, J. Ouyang, F. Yang, W. Han, and L. Zhou, "Multi-element phased array calibration method by solving linear equations," *IEEE Transactions on Antennas and Propagation*, vol. 65, no. 6, pp. 2931–2939, 2017.

[14] F. Zhang, W. Fan, Z. Wang, Y. Zhang, and G. F. Pedersen, "Improved over-the-air phased array calibration based on measured complex array signals," *IEEE Antennas and Wireless Propagation Letters*, vol. 18, no. 6, pp. 1174–1178, 2019.